Research Square

Preprints are preliminary reports that have not undergone peer review.
They should not be considered conclusive, used to inform clinical practice,
or referenced by the media as validated information.

An Investigation of the Complexes of Host Compound N,N'-Bis(5-phenyl-5-dibenzo[a,d]cycloheptenyl)hexane-1,6-diamine with Guest Solvents Aniline, N- Methylaniline and N,N’-Dimethylaniline

Benita Barton

benita.barton@mandela.ac.za

Nelson Mandela University

Jarryd A. Vorgers

Nelson Mandela University

Eric C. Hosten

Nelson Mandela University

Research Article

Keywords: Host–guest, aniline, NMA, DMA, crystal structure, thermal stability.

Posted Date: November 12th, 2026

DOI: https://doi.org/10.21203/rs.3.rs-11536894/v1

License: This work is licensed under a Creative Commons Attribution 4.0 International License.
Read Full License

Additional Declarations: No competing interests reported.

Abstract

In the present investigation, *N*,*N*′-bis(5-phenyl-5-dibenzo[a,d]cycloheptenyl)hexane-1,6-diamine (**H**) was demonstrated to have host ability for aniline (ANI), *N*-methylaniline (NMA) and *N*,*N*-dimethylaniline (DMA), enclathrating each one consistently with 2:1 host:guest (H:G) ratios, as observed through ^{1}H-NMR experiments. Single crystal X-ray diffraction (SCXRD) analyses showed that these complexes crystallised in the triclinic crystal system and space group *P*$\bar{1}$, and that 2**H**·ANI and 2**H**·NMA shared a common host packing motif in the unit cell; this packing was unique in the DMA-containing inclusion compound. These experiments also revealed that only ANI and NMA experienced stabilizing close contacts with **H**, of the (host)C–H···π(guest) type, and that the guest molecules were located in discrete cavities; DMA, on the other hand, was housed in infinite and open channels, and was retained in the crystals of the complex through steric factors alone and did not interact with **H** through noncovalent interactions. Expectedly, as a result, thermal analyses on the three complexes demonstrated that 2**H**·ANI possessed the greater thermal stability, followed by 2**H**·NMA, while the DMA-containing inclusion compound was least stable. Finally, by means of guest competition experiments, **H** was shown to possess selectivity for, unsurprisingly, ANI. However, the observed selectivity was only modest, and **H** does not possess the ability to separate these binary mixtures through host–guest chemistry protocols.

1. Introduction

Host–guest chemistry is a sub-category of the much broader supramolecular chemistry area of science, and relies upon the existence of noncovalent interactions between, more usually, different molecular entities [1, 2]. These stabilizing close contacts may include classical and nonclassical hydrogen bonding, π stacking events, X–H···π interactions and van der Waals forces, to mention only a few, which facilitate the formation of inclusion complexes comprised of the host and guest species. The stereoelectronic alignment of the binding sites in the host and guest molecules are complementary, and host molecules are defined to possess binding sites that are convergent, while those of the guest are divergent in nature [3].

The literature is abound with an overwhelming number of reports that recognize the very many important applications of host–guest chemistry, including drug solubility, stability and delivery [4–7], wastewater remediation and environmental cleanup [8–10], chemosensing [11–13], the resolution of racemic mixtures [14], and the separation of other types of isomers (positional, *etc*.) and related compounds that possess near-identical physical properties [15–18]. In fact, in 2016, Sholl and Lively reported in *Nature* that there exist seven chemical separations that would change the world if devised to be more energy efficient than current separation strategies [19]. In our own laboratories, we have focussed on, more usually, the separation of positional isomers and related compounds through host–guest chemistry protocols with much success. As an example, the host compound bearing a roof-shaped design, *trans*-9,10-dihydro-9,10-ethanoanthracene-11,12-dicarboxylic acid, was demonstrated to have a near-complete selectivity for *p*-dichlorobenzene when crystallized from various mixtures containing also the *ortho*- and/or *meta*-isomers [20]. The same host species was also capable of effecting separations of mixtures

of anisole and the bromoanisoles and, furthermore, the methylanisoles [21, 22]. Additionally, *N*,*N*'-bis(9-phenyl-9-xanthenyl)butane-1,4-diamine, prepared from xanthone, was revealed to have the ability to selectively enclathrate either *ortho*- or *para*-xylene when presented with mixtures of the C_8H_{10} aromatic fraction of crude oil [23]. Moreover, *N*,*N'*-bis(9-(4-fluorophenyl)-9-xanthenyl)ethylenediamine, also derived from xanthone, possessed separation capability in pyridine and methylpyridine solutions [24]. One final example is 9,9'-bifluorenyl-9,9'-diol, synthesized from fluorenone [25], which was demonstrated to have an enhanced affinity for *N*-methylaniline when crystallized from aniline/*N*-methylaniline/*N*,*N*-dimethylaniline solutions that present as mixtures as a result of synthetic *N*-methylation protocols of aniline [26–33].

In the present investigation, the host compound *N*,*N'*-bis(5-phenyl-5-dibenzo[a,d]cycloheptenyl)hexane-1,6-diamine (**H**) was assessed for its host ability for these aniline (ANI), *N*-methylaniline (NMA) and *N*,*N*-dimethylaniline (DMA) solvents, the results of which have not been declared in the literature before. This host compound, however, has been shown to have the ability to form complexes with cyclohexanone and methylcyclohexanones [34] and, more significantly, to possess substantial selectivities towards *o*-xylene when crystallized from a variety of xylene/ethylbenzene mixtures, so much so that separations of such mixtures were shown to be plausible on an industrial scale [35]. In the present work, any resulting complexes were closely scrutinised by means of both single crystal X-ray diffraction (SCXRD) and thermoanalytical experiments. The first of these techniques assisted in determining the crystal systems and space groups applicable to the resultant crystals of the inclusion compounds, their space groups and, furthermore, the noncovalent interactions responsible for guest retention. The latter technique (thermal analysis) was applicable in order to observe the relative thermal stabilities of the complexes through a consideration of the onset temperatures (T_{on}) of the guest release events. For the sake of completeness, the selectivity of **H** was also assessed by means of crystallisation experiments from a variety of different guest solutions to ascertain whether **H** has the ability to separate such mixtures, the components of which boil within a very narrow temperature range, ensuring challenging separations through the more conventional fractional distillations. We report on all of these results now.

2. Experimental

2.1 General

The starting materials towards the synthesis of **H** were purchased from Merck (South Africa), as were the potential guest solvents ANI, NMA and DMA. These were used as received.

^{1}H-NMR experiments were carried out in $CDCl_3$; the applicable instrument was a Bruker Ultrashield Plus 400 MHz NMR spectrometer and data were analysed using TopSpin 4.4.1 software.

Single crystal X-ray diffraction (SCXRD) experiments were carried out by means of a Bruker D8 Quest diffractometer with a Photon II CPAD detector and IμS 3.0 Mo source (Kα, λ = 0.71073 Å). APEX5 software facilitated diffraction data acquisition, while SAINT and SADABS were employed for cell

refinement and data reduction, as well as multi-scan adsorption corrections, respectively [36, 37]. The crystal structures were solved using the dual-space method of SHELXT-2018/2 [38] with subsequent least-squares refinement carried out in SHELXL-2025/1 [39]. The SHELXLE [40] graphical user interphase enabled structural visualization, and molecular diagrams were generated using ORTEP-3 for Windows (version 2023.1) (in the Supplementary Information, SI) [41]. Anisotropic refinement was applied to all non-hydrogen atoms. Carbon-bound hydrogen atoms were positioned as per standard geometric constraints (C–H bond lengths: 0.95 Å for aromatic carbons, 1.00 Å for methine, and 0.99 Å for methylene) and refined by means of the riding model approximation, with U_{iso}(H) fixed at 1.2U_{eq}(C). Rotational freedom about the C–C bond was permitted for non-disordered methyl hydrogen atoms in order to best match the experimental electron density (HFIX 137 in the SHELXL [39] program); C–H bond lengths were restrained to 0.98 Å and U_{iso}(H) parameters fixed at 1.5U_{eq}(C). Nitrogen-bound hydrogen atoms were located on the difference Fourier maps and refined freely whenever possible; otherwise, these were positioned geometrically and refined with a riding model (N–H bond lengths were restrained to 0.88 Å and U_{iso}(H) fixed at 1.2U_{eq}(N)). The crystal structures of 2**H**·ANI, 2**H**·NMA and 2**H**·DMA were deposited at the Cambridge Crystallographic Data Centre (CCDC), and their deposition numbers are 2582100, 2582101 and 2582102, respectively.

Gas chromatography (GC) analysis was performed using an Agilent Technologies 7890A GC coupled to a flame ionisation detector (FID). The applicable stationary phase was an Agilent J&W Cyclosil-B column. Samples were dissolved in dichloromethane prior to injection. The oven program commenced at 50°C (with no initial hold time) which was then ramped up at a rate of 15°C·min^{-1} to attain a final temperature of 200°C, where it was maintained for 1 min. The split ratio was 1:100 and the helium carrier gas flow rate 1.5 mL·min^{-1}.

2.2 Synthesis of *N*,*N'*-bis(5-phenyl-5-dibenzo[a,d]cycloheptenyl)hexane-1,6-diamine (H).

The host species (**H**) was synthesized through consideration of a previous report [42].

2.3 The host ability of H for each of ANI, NMA and DMA using crystallization experiments

In order to determine whether **H** has the ability to form complexes with ANI, NMA and DMA, this host compound was crystallised from each of these potential guest solvents in glass vials. This was achieved by dissolving **H** (0.05 g, 0.08 mmol) in an excess of each one, employing mild heat to ensure complete host dissolution. The vials were left open to the ambient conditions which assisted in the formation of crystals. These were collected under suction, washed with low boiling petroleum ether and analysed by means of ^{1}H-NMR spectroscopy. If complexation had been successful, both host and guest resonance signals were present on the resultant NMR spectra (these have been deposited in the SI). The host:guest (H:G) ratios were calculated by integrating and comparing the areas under appropriate host and guest signals.

2.4 The host selectivity behaviour when crystallized from various solutions containing ANI/NMA/DMA mixed in equimolar proportions

The selectivity behaviour of **H** was subsequently investigated through crystallisation experiments from mixed guest solutions, where guests were present in equimolar proportions; all possible guest combinations were considered. Therefore, **H** (0.05 g, 0.08 mmol) was dissolved in the prepared equimolar guest mixtures (1–2 mmol combined amount) and the vials were closed and left at ambient conditions. The crystals that formed in this way were isolated and treated as before, and analysed by means of ^{1}H-NMR spectroscopy, to obtain the overall H:G ratios, and GC, for the quantification of the guests in any mixed guest complexes.

2.5 The host selectivity behaviour when crystallized from binary solutions containing ANI/NMA/DMA mixed in different molar ratios

Following this, **H** (0.05 g, 0.08 mmol) was crystallised from binary guest mixtures (1–2 mmol combined amount) in which Guest A (G_A) and Guest B (G_B) were present in 20:80, 40:60, 60:40 and 80:20 molar proportions, to observe the host selectivity behaviour in such conditions. These experiments were carried out in the same manner as the equimolar mixed guest crystallisations. Crystals were analysed using GC for guest quantification purposes. It was then possible to construct selectivity profiles in which the mole fraction of G_A (or G_B) in the crystalline phase (Z_A or Z_B) was plotted against the amount of G_A (or G_B) in the original solution (X_A or X_B), according to the equation of Pivovar and coworkers, $K = Z_B/Z_A \times X_A/X_B$, where $X_A + X_B = 1$ [43]. These profiles provide a visual means of observing the host selectivity behaviour in these conditions. The selectivity coefficient, K, serves as a measure of this selectivity, with K = 1 representing a host compound that does not have an affinity for either guest species present. This scenario (K = 1) is represented by the straight diagonal lines that have been inserted into each plot for facile comparison purposes with the experimentally obtained data points. Efficient separations on an industrial platform of such binary mixtures are plausible when K is 10 or greater, as reported by Nassimbeni *et al* [44, 45].

2.6 Software

Program Mercury [46] was employed to analyse the crystal structures obtained from the SCXRD experiments. In this manner, unit cell, host and host–guest packing, noncovalent interaction and void diagrams were thus prepared. In the latter instance, the guest molecules were deleted from the packing calculations and the spaces that formed as a result were analysed by means of a probe with a radius of 1.2 Å.

3. Results and discussion

3.1 The host ability of H for each of ANI, NMA and DMA using crystallization experiments

When **H** was crystallised independently from each of ANI, NMA and DMA, inclusion compounds were formed in each case. The host:guest (H:G) ratios, obtained from ^{1}H-NMR experiments, were consistently 2:1. (These spectra have been placed in the Supplementary Information (SI) section.)

3.2 Single crystal X-ray diffraction

Each of the three complexes was subjected to analysis through SCXRD experiments and Table 1 contains the relevant crystallographic data that were obtained in each instance. Note that in the case of the 2**H**·DMA complex, the first crystal that was selected fractured at 200 K, and so the experiment was repeated at 278 K instead in order to obtain the crystal structure. These inclusion compounds crystallised in the triclinic crystal system and space group *P*$\bar{1}$. The unit cell dimensions in each of 2**H**·ANI and 2**H**·NMA were comparable, suggesting isostructural host packing assemblies, which was confirmed by means of simulated powder XRD patterns, as depicted in Figs. 2a and b; this packing in the complex with DMA was, however, unique (Fig. 2c). Interestingly, the complexes of **H** with cyclohexanone and each of the three methylcyclohexanone isomers [34] also demonstrated very similar unit cell dimensions and host packing motifs as was noted in 2**H**·ANI and 2**H**·NMA.

Table 1
Crystallographic data for the complexes of **H** with ANI, NMA and DMA.

Chemical formula	**2H·ANI**	**2H·NMA**	**2H·DMA**
	$2C_{48}H_{44}N_2·C_6H_7N$	**$2C_{48}H_{44}N_2·C_7H_9N$**	**$2C_{48}H_{44}N_2·C_8H_{11}N$**
Formula weight	1390.82	1404.85	1418.88
Crystal system	Triclinic	Triclinic	Triclinic
Space group	*P*□1	*P*□1	*P*□1
μ (Mo-Kα)/mm^{-1}	0.070	0.070	0.067
3)a/Å	10.7754(5)	10.9309(9)	9.8768(11)
b/Å	12.5797(6)	12.5572(9)	12.7511(12)
c/Å	15.8620(6)	15.8344(13)	17.762(2)
alpha/°	73.144(2)	71.076(3)	90.179(4)
beta/°	85.728(2)	86.500(3)	104.479(4)
gamma/°	67.308(2)	69.473(3)	110.275(2)
V/$Å^3$	1896.75(15)	1922.0(3)	2021.8(4)
Z	1	1	1
F(000)	742	750	758
Temp./K	200	200	278
Restraints	118	51	146
Nref	8032	7052	8881
Npar	554	520	569
R	0.0634	0.0866	0.1255
wR2	0.1606	0.1742	0.1878
S	1.16	1.24	1.32
θmin–max/°	1.9, 26.7	2.2, 25.4	2.0, 27.1
Tot. data	120184	85426	124215
Unique data	8032	7052	8881
Observed data [I > 2.0 sigma(I)]	5582	5644	6172
R_{int}	0.049	0.111	0.087

Chemical formula	2H·ANI	2H·NMA	2H·DMA
	$2C_{48}H_{44}N_2·C_6H_7N$	$2C_{48}H_{44}N_2·C_7H_9N$	$2C_{48}H_{44}N_2·C_8H_{11}N$
Completeness	1.000	0.998	0.999
Min. resd. dens./e·Å^{-3}	−0.29	−0.37	−0.22
Max. resd. dens./e·Å^{-3}	0.28	0.58	0.36
Density/g·cm^{-3}	1.218	1.214	1.165
CCDC numbers	2582100	2582101	2582102

Figures 3a (for 2**H**·ANI, representing also isostructural 2**H**·NMA) and b are depictions of the host–guest packing and unit cells (left) and the guest accommodation type (right). These clearly demonstrate that the guest molecules in 2**H**·ANI and 2**H**·NMA resided in discrete and isolated cages while the DMA molecules were located in infinite unidirectional channels.

The host molecules in the three complexes did not possess symmetry of any kind. Moreover, the carbon atoms in each of the 1,6-diaminohexane linking chains in the complexes with ANI and DMA experienced positional disorder, with site-occupancy factors (s.o.f.s) 0.56:0.44 and 0.51:0.49, respectively. On the other hand, the guest molecules were all disordered around an inversion point.

A close scrutiny of the noncovalent interactions present in the three complexes was subsequently undertaken. Surprisingly, given the number of aromatic moieties in each one, no significant π···π interactions were present between or within any of the molecular entities. Additionally, despite the host and guest molecules possessing the ability for engaging in classical hydrogen bonding, these types of short contacts were also absent in all three inclusion compounds. However, intramolecular non-classical hydrogen bonds of the (host)C–H···N(host) type were identified, numbering four in each complex, and involving all four of the fused aromatic ring systems of each host molecule, while the free phenyl rings did not interact in this manner. These interactions measured 2.36–2.40 Å (H···N) and 2.747(3)–2.774(3) Å (C···N) (2**H**·ANI), 2.35–2.41 Å (H···N) and 2.733(4)–2.773(4) Å (C···N) (2**H**·NMA), and 2.36–2.38 Å (H···N) and 2.733(8)–2.760(6) Å (C···N) (2**H**·DMA); angles were expectedly small (given their intramolecular nature), measuring between 102 and 104°. These close contacts served to stabilize the host molecular geometry in the unit cell in each instance.

While no short contacts of any type between the host and guest molecules could be identified in the complex with DMA, both ANI and NMA were involved in (host)C–H···π(guest) stabilizing contacts, numbering two in each complex and involving the linker diaminohexane sp^3 C–H groups. Dimensions were 3.00 Å, 2.96 Å (H···π), 3.529(8) Å, 3.605(7) Å (C···π), 115°, 124° (2**H**·ANI), and 2.93 Å, 2.99 Å (H···π), 3.781(6) Å, 3.680(6) Å (C···π), 144°, 127° (2**H**·NMA). These interactions facilitated the retention of the ANI and NMA guest molecules in the crystals of their complexes with **H**.

It may be expected that, since DMA did not experience any close contacts with **H** and was located in wide open channels, the complex 2**H**·DMA would release its guest molecules at a lower temperature relative to 2**H**·ANI and 2**H**·NMA, since ANI and NMA were stabilized in their complexes by means of (host)C–H···π(guest) interactions and these guests also resided in isolated cages. It is therefore predicted that the 2**H**·DMA would have the lower relative thermal stability of the three complexes. In order to assess whether this projection is correct, the three complexes were subsequently subjected to a controlled heating program, through thermoanalytical experiments.

3.3 Thermal analysis

After heating the three complexes from approximately 40°C to 350°C, the overlaid thermal curves (the differential scanning calorimetry (DSC, blue), thermogravimetry (TG, red), and its derivative (DTG, green)), as provided in the SI section, were obtained. Table 2 contains a summary of the relevant data obtained from these curves, namely the onset temperature of the guest release event (T_{on}, a measure of the relative thermal stability of the complex), the endotherm peak temperature of the host melt (T_p), and the measured mass loss experienced by the complex upon complete removal of the guest species. Also provided in this table are the calculated mass loss percentages expected for these 2:1 H:G complexes for facile comparisons with the measured percentages.

Table 2
Thermal properties of the three aniline complexes with **H**.

Complex	T_{on}[a] /°C	T_p[b] /°C	Measured mass loss /%	Expected mass loss /%
2**H**·ANI	108.9	199.4	7.0	7.0
2**H**·NMA	104.4	199.1	7.9	8.0
2**H**·DMA	97.6	198.9	10.8	8.5

[a] Estimated from the DTG curves.

[b] The endotherm peak temperature of the melting event of the host compound.

From these thermal curves (Figures S3a–c, SI), the guest loss of the three complexes upon heating occurred in a single step spanning a broad temperature range, and their relative thermal stabilities were observed to be in the order 2**H**·ANI (T_{on} 108.9°C) > 2**H**·NMA (104.4°C) > 2**H**·DMA (97.6°C). These observations are in complete agreement with the results from the SCXRD experiments, where DMA experienced no close contacts with **H** and, additionally, resided in channels, resulting in its lower thermal stability relative to the complexes with ANI and NMA, which did experience stabilizing interactions with **H** and which were located in discrete voids (a characteristic associated with higher relative thermal stabilities compared with channel occupation). The endotherm peak temperature for the host melt event was noted to be between 198.9 and 199.4°C, which correlated with another report (190.2–196.4°C) [35].

Finally, the measured and calculated mass losses for complete guest removal from each complex concurred reasonably well (2**H**·ANI, 7.0 vs 7.0%, 2**H**·NMA, 7.0 vs 8.0% and 2**H**·DMA, 10.8 vs 8.5%).

3.4 The host selectivity behaviour when crystallized from various solutions containing ANI/NMA/DMA mixed in equimolar proportions

Owing to ANI/NMA/DMA presenting as mixtures during the synthesis of the methylated anilines from ANI [26–33], for the sake of completeness, it was deemed appropriate to investigate whether **H** has the ability to separate such mixtures through host–guest chemistry strategies. The more conventional fractional distillation techniques are presently challenging for this purpose in that these anilines boil within a narrow temperature range (184–194°C). This investigation was further encouraged by the consideration of a previous report in which **H** was demonstrated to possess the ability to separate the C_8H_{10} isomers of crude oil, namely the three xylenes and ethylbenzene, through host–guest chemistry protocols [35].

As such, when **H** was crystallised from equimolar mixed aniline guest solutions, the results as contained in Table 3 were obtained. Here, preferred guests are highlighted by means of red bold text. These experiments were conducted in duplicate to confirm their repeatability and so the percentage estimated standard deviations (% e.s.d.s) are also provided in this table.

Table 3
The results of the equimolar mixed guest experiments.

ANI	NMA	DMA	G:G	% e.s.d.s
X	X		**83.9**:16.1	2.6
X		X	**53.9**:46.1	0.7
	X	X	*a*	*a*
X	X	X	**61.5**:7.3:31.2	1.4:1.3:2.8

[a] Did not crystallise.

These results (Table 3) suggest that **H** does indeed possess selectivity when crystallised from equimolar ANI/NMA/DMA solutions, always favouring ANI in these conditions. The ANI/NMA experiment furnished crystals with a significantly elevated quantity of ANI (83.9%), while this selectivity was more modest (53.9%) but remained for ANI in the ANI/DMA solution. Interestingly, despite an extended period of time (months), the NMA/DMA experiments (that is, in the absence of preferred ANI) did not afford any crystals whatsoever. Finally, the equimolar ternary mixture too produced a solid enriched in ANI (61.5%). In fact, the selectivity of the host compound in these experiments was shown to be in the order ANI > DMA > NMA, with NMA being consistently disfavoured throughout. It is not unexpected that ANI was the preferred guest solvent, given the increased thermal stability of 2**H**·ANI (from thermal analysis) and that

ANI was retained in the crystals of its complex through close contacts with the host species in closed cavities (from SCXRD). Contrarily, however, the higher selectivity observed for DMA relative to NMA in these solutions was unexpected, since NMA also experienced close contacts with **H** and was similarly housed in discrete voids, whilst DMA did not interact with **H** and was located in channels and its complex was the least stable one. A plausible explanation for this perceived anomalous behaviour is that the selectivity of **H** was obtained through mixed-guest crystallisation experiments while thermal experiments (and SCXRD) were performed on the single-guest solvent complexes. It should therefore not be expected that the results from all three sets of experiments always correlate since the behaviour of the host compound is compared in, essentially, different experimental conditions (multiple *vs* single-guest conditions).

3.5 The host selectivity behaviour when crystallized from binary solutions containing ANI/NMA/DMA mixed in different molar ratios

The selectivity of **H** was also examined in binary guest solutions containing guest solvents in varying proportions. The selectivity profiles obtained from these crystallisation experiments are provided in the SI, and the K values calculated for each data point are summarised in Table 4.

Table 4

The K values for each data point in the selectivity profiles.[a]

	K value (in favour of)			
Solution	**20:80**	**40:60**	**60:40**	**80:20**
ANI/NMA	**8.7 (ANI)**	**4.6 (ANI)**	**2.8 (ANI)**	**1.9 (ANI)**
ANI/DMA	**7.5 (ANI)**	**3.0 (ANI)**	**1.5 (ANI)**	**1.5 (DMA)**

[a] All of the NMA/DMA experiments failed to produce any crystals despite extended periods of time; the selectivity profile for these experiments could thus not be constructed and nor could the K values, therefore, be calculated.

The highest K value (8.7) that was obtained was in the 20:80 ANI/NMA experiment, unsurprisingly favouring ANI, followed by the 20:80 ANI/DMA experiment (7.5), also in favour of ANI (Table 4). All remaining K values were low, ranging between 1.9 and 4.6 (ANI/NMA), and 1.5 and 3.0 (ANI/DMA). All experiments demonstrated that ANI was the preferred guest of **H**, with one exception, the 80:20 ANI/DMA experiment, in which DMA was then marginally favoured (K 1.5).

These K values suggest that efficient separations of such binary mixtures on an industrial platform, through host–guest chemistry strategies, are generally not viable given that K is required to be 10 or

greater for effectivity, as reported by Nassimbeni and coworkers [44, 45].

4. Conclusions

Here, *N*,*N*′-bis(5-phenyl-5-dibenzo[a,d]cycloheptenyl)hexane-1,6-diamine (**H**) was shown to function as a host compound for guest solvents aniline (ANI), *N*-methylaniline (NMA), and *N*,*N*-dimethylaniline (DMA); H:G ratios were consistently 2:1. SCXRD analysis revealed that the three complexes each crystallised in the triclinic crystal system with space group *P*$\bar{1}$. Moreover, 2**H**·ANI and 2**H**·NMA exhibited a common host packing arrangement that differed from the packing observed in the DMA-containing complex. The crystal structures further showed that only ANI and NMA formed stabilising (host)C–H···π(guest) interactions with the host species and that guests were located in discrete cavities. In contrast, DMA occupied infinite and wide-open channels and was retained primarily through steric confinement rather than specific noncovalent interactions with **H**. Consistent with these observations, thermal analysis demonstrated that 2**H**·ANI was the most thermally stable complex, followed by 2**H**·NMA, whereas the DMA inclusion compound exhibited the lowest thermal stability. Guest competition experiments further revealed that **H**, unsurprisingly, possessed a clear preference for ANI, but the observed host selectivity was not noteworthy enough to suggest that **H** is able to separate any of these binary guest solutions by means of host–guest chemistry strategies.

Declarations

Supplementary information

The crystal structures of 2**H**·ANI, 2**H**·NMA and 2**H**·DMA were deposited at the Cambridge Crystallographic Data Centre (CCDC), and their deposition numbers are 2582100, 2582101 and 2582102, respectively. These data are freely accessible at www.ccdc.cam.ac.uk/structures/. The ORTEP diagrams, ^{1}H-NMR spectra of the three complexes, their thermal curves and the selectivity profiles may also be found in this section.

Conflict of interest

There are no conflicts of interest to declare.

Author Contribution

B.B.: conceptualization; methodology; funding acquisition; project administration; resources; supervision; visualization; writing the original draft. J.A.V.: investigation; methodology; validation; compiling all results. E.C.H.: data curation; formal analysis.

Acknowledgement

Financial support is acknowledged from the Nelson Mandela University and the National Research Foundation (NRF) of South Africa.

Data Availability

The crystal structures of 2H·ANI, 2H·NMA and 2H·DMA were deposited at the Cambridge Crystallographic Data Centre (CCDC), and their deposition numbers are 2582100, 2582101 and 2582102, respectively. These data are freely accessible at www.ccdc.cam.ac.uk/structures/.

References

1. Lehn, J.-M.: *Supramolecular Chemistry Concepts and Perspectives*, VCH Verlagsgesellschaft mbH, Weinheim (Bundesrepublik Deutschland), 1st edn., (1995)
2. Steed, J.W., Atwood, J.L.: *Supramolecular Chemistry*, Wiley, 3rd Edn., (2022)
3. Biedermann, F., Schneider, H.J.: Experimental binding energies in supramolecular complexes. Chem. Rev. **116**, 5216–5300 (2016)
4. Sahu, K.M., Patra, S., Swain, S.K.: Host-guest drug delivery by β-cyclodextrin assisted polysaccharide vehicles: A review. Int. J. Biol. Macromol. **240**, 124338 (2023)
5. Colaco, V., Jadhav, S.R., Bandi, S.P., Datta, D., Dhas, N., Thakur, G., Ramesh, B.V., Alizadeh, B.: Multifunctional application of supramolecular cucurbiturils as encapsulating hosts in drug delivery: A review. Int. J. Pharm. **681**, 125801 (2025)
6. Tang, Y., Mao, Y., Wang, L., Ding, Y.-F., Li, P., Xie, B.: Mater. Today Bio. **37**, 102901 (2026)
7. Chen, A., Peng, Y., Chen, Z., Lu, Y., Guo, M., Cai, T.: Crystal engineering for poorly water-soluble drugs: From design to applications. Acta Pharm. Sin B. **16**, 1848–1882 (2026)
8. Omrani, S., Ghasemi, M., Tan, H.L., Thi, Q.V., Niasar, V., Truong, V.X.: Sustain. Mater. Technol. **45**, e01592 (2025)
9. Panda, P., Panda, T.: Imide-based covalent organic frameworks: Molecular design, synthesis, and applications in clean energy and environmental remediation. RSC Adv. **15**, 43013–43027 (2025)
10. Zhang, X., Chen, R., Wang, X., Tong, Y., Zhao, S., Ang, E.H., Silanpää, M.: CD-enabled supramolecular platforms for cleaner production: From deep eutectic solvents to membranes and extraction. Coord. Chem. Rev. **562**, 217963 (2026)
11. Moral, R., Das, G.: An expedition towards designing of luminescent supramolecular metallogels for chemosensing applications. Inorg. Chim. Acta. **581**, 122635 (2025)
12. Iskierko, Z., Noworyta, K., Sharma, P.S.: Molecular recognition by synthetic receptors: Application in field-effect transistor based chemosensing. Biosens. Bioelectron. **109**, 50–62 (2018)

13. Li, M., Wen, F., Jiang, Y.-N., Sun, N., Xing, S., Wang, B.: Emerging trends in cucurbit[*n*]uril-based sensing. Coord. Chem. Rev. **542**, 216870 (2025)
14. Seebach, D., Beck, A.K., Heckel, A.: TADDOLs, their derivatives, and TADDOL analogues: Versatile chiral auxiliaries. Angew Chem. Int. Ed. **40**, 92–138 (2001)
15. Boudiombo, J.S.B., Su, H., Bourne, S.A., Weber, E., Nassimbeni, L.R.: Separation of lutidine isomers by selective enclathration. Cryst. Growth Des. **18**, 2620–2627 (2018)
16. Zhao, K., Zeng, J., Liu, M., Wang, Y., Peng, Y., Yang, Y., Zheng, K., Wang, Z., Xi, H., Duan, C.: Recent advances in metal–organic frameworks for xylene isomers separation: Performance and mechanism insights. Green. Technol. Sustain. **4**, 100390 (2026)
17. Zhang, G., Ding, Y., Hashem, A., Fakim, A., Khashab, N.M.: Xylene isomer separations by intrinsically porous molecular materials. Cell. Rep. Phys. Sci. **2**, 100470 (2021)
18. Wu, N., He, S., Ding, H., Wu, F., Xiao, Y., Ding, L., Ding, C.-F.: Differentiation of positional isomers of branched-chain fatty acids using ion mobility-mass spectrometry based on host-guest chemistry. Food Chem. **509**, 148516 (2026)
19. Sholl, D., Lively, R.: Seven chemical separations to change the world. Nature. **532**, 435–437 (2016)
20. Barton, B., Caira, M.R., Senekal, U., Hosten, E.C.: *trans*-9,10-Dihydro-9,10-ethanoanthracene-11,12-dicarboxylic acid: Complete host selectivity for guest compound *para*-dichlorobenzene during crystal growth from mixed isomeric dichlorobenzenes, *Cryst. Growth Des. 22*, 3385–3394. (2022)
21. Barton, B., Caira, M.R., Senekal, U., Hosten, E.C.: *trans*-9,10-Dihydro-9,10-ethanoanthracene-11,12-dicarboxylic acid: Remarkable host selectivities in the presence of mixtures of anisole and bromoanisole isomers. *Cryst. Growth Des. 23*, 501–510. (2023)
22. Barton, B., Senekal, U., Hosten, E.C.: Host compound DED: Guest accommodation type, non-covalent host···guest interactions, crystal densities and thermal stabilities ensure high host selectivities for 4-methylanisole in anisole and methylanisole mixtures. Cryst. Growth Des. **23**, 602–611 (2023)
23. Barnardo, B., Barton, B., Caira, M.R., Hosten, E.C.: Evaluation of the behaviour of two tricyclic-fused host systems in the presence of single and mixed isomers of the C_8H_{10} aromatic crude oil fraction. Cryst. Growth Des. **24**, 5603–5613 (2024)
24. Trollip, D.B., Barton, B., Caira, M.R., Hosten, E.C.: Effective alternative host-guest separation strategies for mixed pyridine/methylpyridines with thioxanthenyl- and xanthenyl-derived host molecules. J. Incl. Phenom. Macrocycl. Chem. **106**, 139–156 (2026)
25. Groenewaldt, J.-L., Barton, B., Hosten, E.C.: 9,9'-Bifluorenyl-9,9'-diol as an effective purification tool for *N*-methyl- and *N*,*N*-dimethylaniline mixtures through host-guest chemistry protocols. RSC Adv. **16**, 39894–39908 (2026)
26. Kahl, T., Schröder, K.-W., Lawrence, F.R., Marshall, W.J., Höke, H., Jäckh, R., Aniline: Ullmann's Encyclopedia of Industrial Chemistry. John Wiley & Sons, Ltd. (2011)
27. Zinin, N.: Beschreibung einiger neuer organischer basen, dargestellt durch die einwirkung des schwefelwasserstoffes auf verbindungen der kohlenwasserstoffe mit untersalpetersäure. J. Prakt Chem. **1842**, *27*, 140–153

28. Porter, H.K.: The Zinin reduction of nitroarenes. In: Organic Reactions, pp. 455–481. John Wiley & Sons, Ltd. (2011)
29. Groggins, P.H.: Amination by reduction. In: Unit Processes in Organic Synthesis, 5th edn., pp. 129–203. McGraw Hill (1958)
30. Sabatier, P., Hydrogénations: In: Béranger, C. (ed.) La Catalyse en Chimie Organique, vol. 3, p. 60. Librairie Polytechnique, Paris (1913)
31. Brown, O.W., Henke, C.O.: Catalytic preparation of aniline. J. Phys. Chem. **26**, 161–190 (1922)
32. Luque, R., Campelo, J.M., Luna, D., Marinas, J.M., Romero, A.A.: Catalytic performance of Al-MCM-41 materials in the *N*-alkylation of aniline. J. Mol. Catal. A: Chem. **269**, 190–196 (2007)
33. Badr, M.Z.A., Aly, D.M.M.: Molecular rearrangements. Part IV. Aryl (alkyl) amines (1), Thermal rearrangement of *N*-benzyl-*N*-methylaniline. Can. J. Chem. **52**, 293–298 (2011)
34. Barton, B., Caira, M.R., Vorgers, J.A.: Host compound *N*,*N*′-bis(5-phenyl-5-dibenzo[a,d]cycloheptenyl)hexane-1,6-diamine and its complexes with guest solvents cyclohexanone and the three methylcyclohexanones: Crystal structures and thermal stability considerations. *CrystEngComm* (2026). 10.1039/D6CE00701E
35. Vorgers, J.A., Barton, B., Hosten, E.C.: Exceptional selectivities of the host compound *N*,*N*′-bis(5-phenyl-5-dibenzo[a,d]cycloheptenyl)hexane-1,6-diamine towards *o*-xylene in xylene/ethylbenzene guest mixtures. Submitted to *CrystEngComm* 28 July 2026.
36. Bruker: APEX4, SADABS and SAINT. Inc., Madison, Wisconsin, USA (2012). Bruker AXS
37. Bruker, A.: APEX2, SADABS and SAINT. AXS Inc., Madison (WI), USA (2010). Bruker
38. Sheldrick, G.M.: SHELXT-Integrated Space Group and Crystal-Structure Determination. Acta Crystallogr. A. **A71**, 3–8 (2015)
39. Sheldrick, G.M.: Crystal Structure Refinement with SHELXL. Acta Crystallogr. C. **C71**, 3–8 (2015)
40. Hübschle, C.B., Sheldrick, G.M., Dittrich, B., ShelXle: A Qt graphical user interface for SHELXL. J. Appl. Crystallogr. **44**, 1281–1284 (2011)
41. Farrugia, L.J.: WinGX and ORTEP for Windows: An update. J. Appl. Cryst. **45**, 849–854 (2012)
42. Trollip, D.B.: Fused Tricyclic Systems as Host Compounds for the Potential Separation of Isomers and Related Compounds through Supramolecular Chemistry Protocols. Nelson Mandela University (2026)
43. Pivovar, A.M., Holman, K.T., Ward, M.D.: Shape-selective separation of molecular isomers with tunable hydrogen-bonded host frameworks. Chem. Mater. **13**, 3018–3031 (2001)
44. Sykes, N.M., Su, H., Weber, E., Bourne, S.A., Nassimbeni, L.R.: Selective enclathration of methyl- and dimethylpiperidines by fluorenol hosts. Cryst. Growth Des. **17**, 819–826 (2017)
45. Nassimbeni, L.R., Sykes, N.M.: Inclusion compounds: Structure, kinetics and selectivity. Crystallogr. Rev. **28**, 70–96 (2022)
46. Macrae, C., Sovago, I., Cottrell, S., Galek, P., McCabe, P., Padcock, E., Platings, M., Shields, G., Stevens, J., Towler, M., Wood, P.: Mercury 4.0: From visualisation to analysis. Design and prediction. J. Appl.

Crystallogr. **53**, 226–235 (2020)

Figures

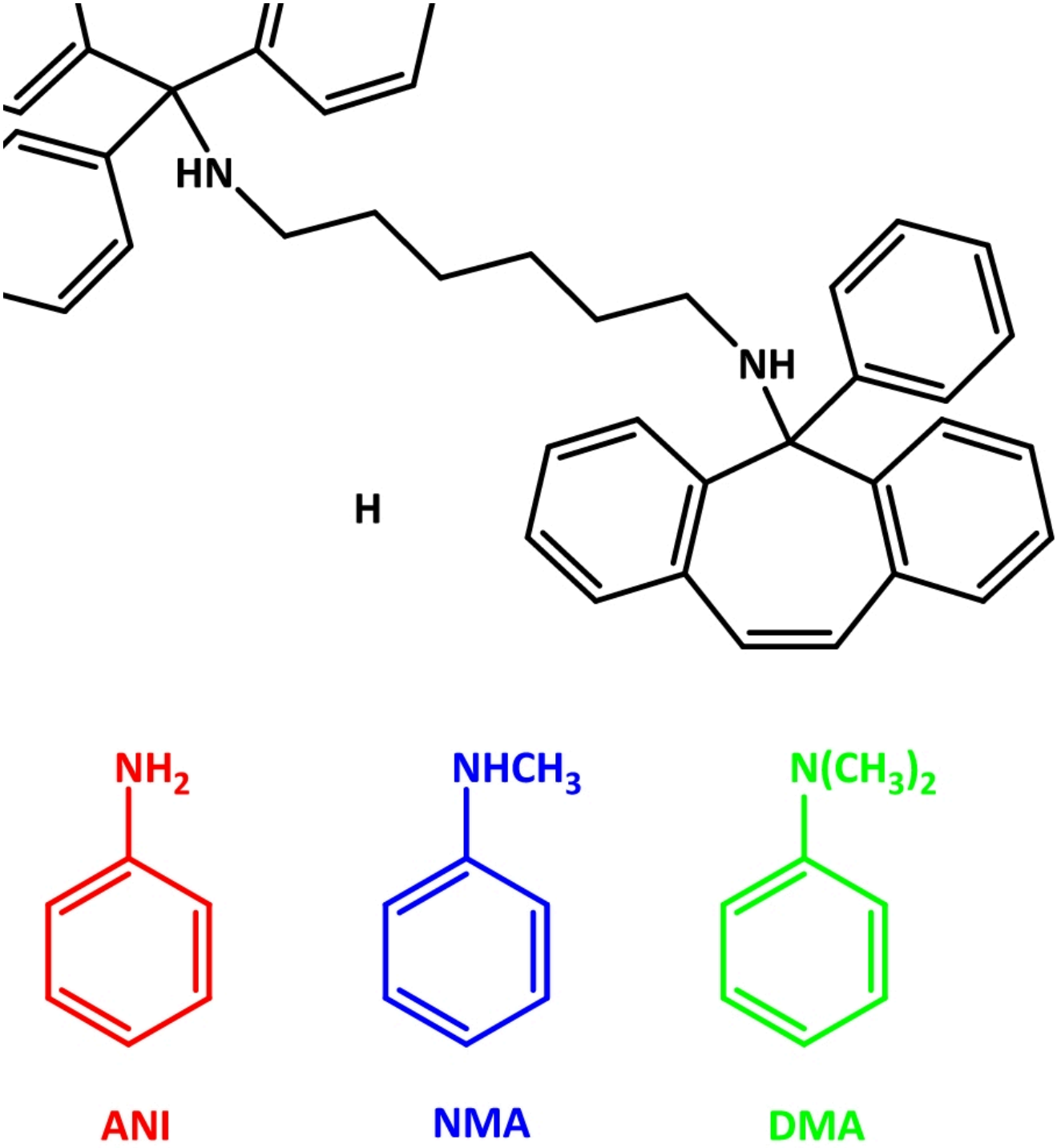


Figure 1

Structures of the host compound, *N*,*N*′-bis(5-phenyl-5-dibenzo[a,d]cycloheptenyl)hexane-1,6-diamine (**H**), and the potential guest solvents aniline (ANI), *N*-methylaniline (NMA) and *N*,*N*-dimethylaniline (DMA).

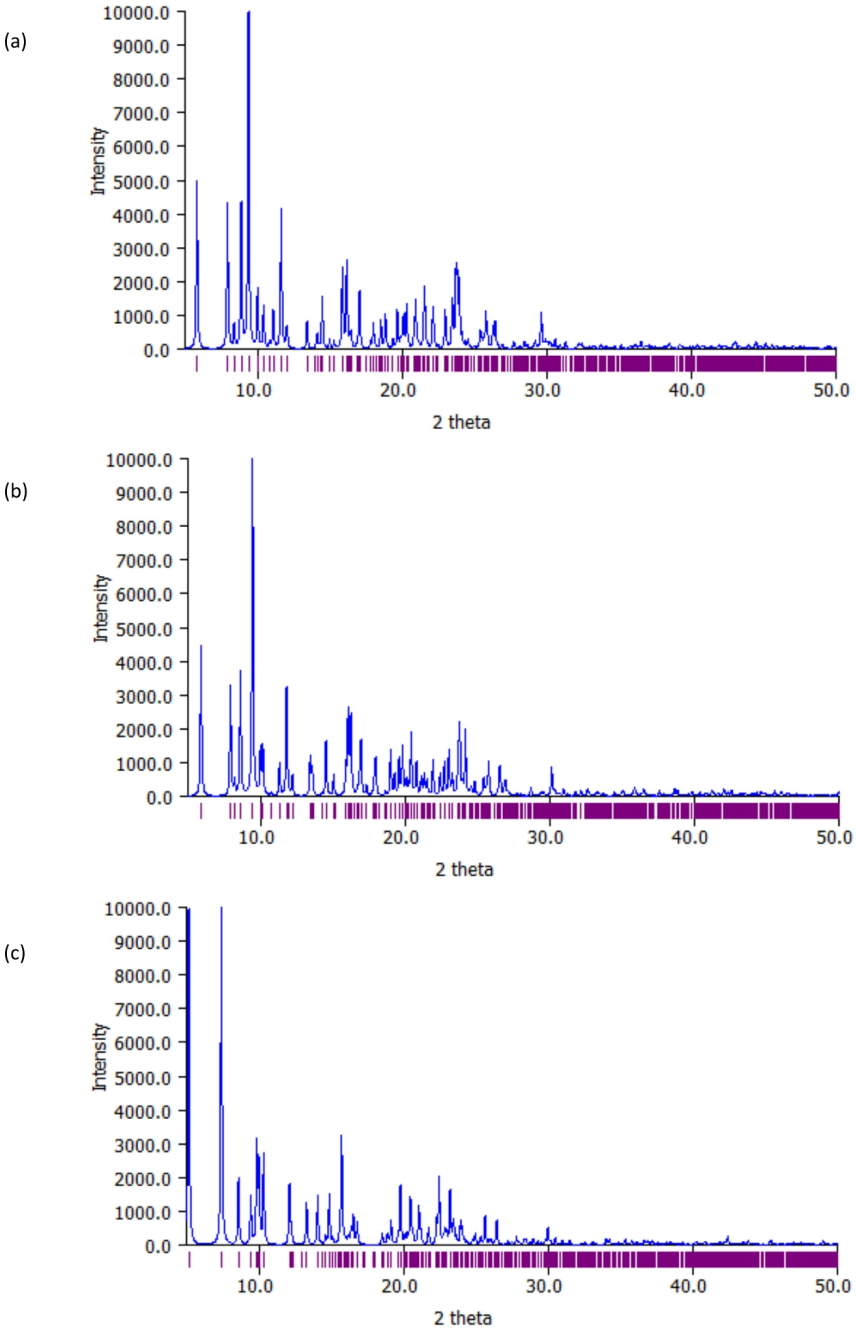


Figure 2

The calculated PXRD patterns ((Cu)Kα) for the host assemblies in (a) 2**H**·ANI, (b) 2**H**·NMA and (c) 2**H**·DMA (after guest deletion from the packing calculations) to indicate the high level of isostructurality

in the complexes containing ANI and NMA; this packing in the DMA complex was different.

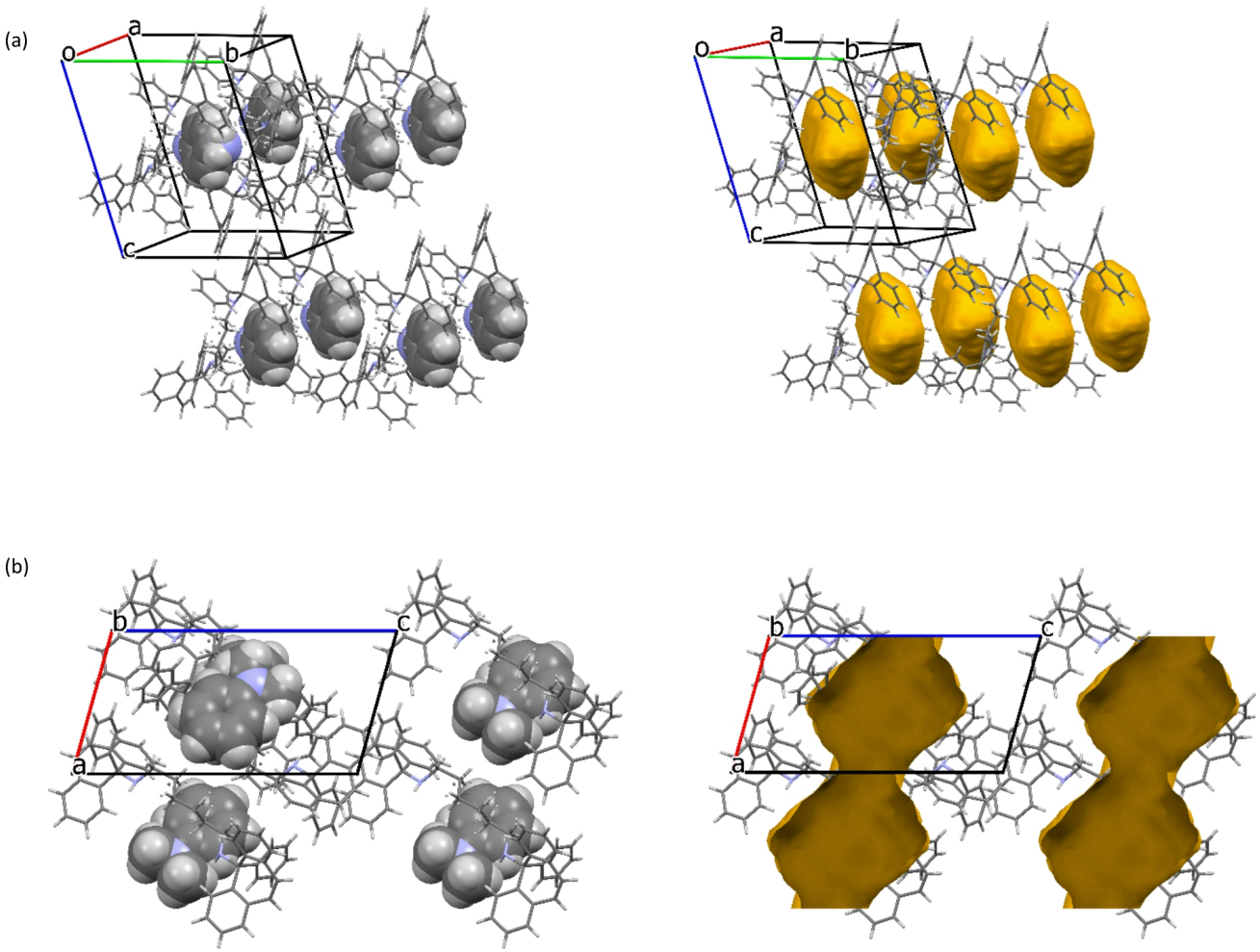


Figure 3

Host–guest packing and unit cells (left) and void diagrams (right) for (a) 2**H**·ANI (representing also isostructural 2**H**·NMA) and (b) 2**H**·DMA.

Supplementary Files

This is a list of supplementary files associated with this preprint. Click to download.

- SUPPLEMENTARYINFORMATION.docx